16th World Congress in Computational Mechanics (WCCM)
21-26 July 2024, Vancouver, Canada
A. Korobenko, M. Laforest, S. Prudhomme, R. Vaziri (Eds)

AN EXPLICIT TIME-MARCHING PROCEDURE FOR ELASTODYNAMIC ANALYSES BASED ON ADAPTIVE TIME-INTEGRATION PARAMETERS AND TIME-STEP VALUES

LUCAS R. PINTO [1], DELFIM SOARES JR.[2], ISABELLE S. SOUZA[1] AND WEBE J. MANSUR[1]

[1]COPPE/Federal University of Rio de Janeiro
CEP 21941-611, Rio de Janeiro, Brazil
lucas.ruffo@engenharia.ufjf.br

[2]Structural Engineering Department, Federal University of Juiz de Fora
CEP 36036-330, Juiz de Fora, MG, Brazil
delfim.soares@ufjf.edu.br

Key words: time-marching, explicit analysis, adaptive parameters, sub-cycling.

Abstract. *This study discusses an explicit time-marching procedure that is designed for the time-domain resolution of elastodynamic models considering their physical properties and adopted spatial discretizations. The technique is entirely automated and proves itself to be highly effective, featuring second-order accuracy, adaptive algorithmic dissipation and extended stability limits. Additionally, the discussed methodology is truly explicit, truly self-starting, and it incorporates automated subdomain/sub-cycling splitting procedures to enhance its overall performance. Thus, the algorithm automatically divides the domain of the problem into different subdomains, adjusting their time-step values according to the properties of the discretized model, which allows improving the efficiency and the accuracy of the analysis, while ensuring stability. Locally-defined adaptive time-integration parameters are also considered, establishing an entirely self-adjustable formulation. In this case, expressions for the time-integration parameters are provided based on the local features of the discrete model, allowing to create a further link between the adopted temporal and spatial discretization procedures, better counterbalancing their errors. These parameters are locally formulated to nullify the bifurcation spectral radius of the method at pre-established sampling frequencies, providing maximal numerical damping at the highest sampling frequency of the elements of the adopted spatial discretization. This design optimizes the formulation to mitigate the influence of spurious high-frequency modes on the computed responses, allowing for enhanced analyses. In fact, the primary goal of introducing numerical damping is to eliminate non-physical spurious oscillations that may arise from the excitation of spatially unresolved modes. Therefore, the methodology not only tracks down the frequency range of the discretized model, but also it is designed to adaptively enforce significantly low values (close to zero) for the spectral radius of the method at the highest frequencies of the model, as well as it aims to provide relatively high spectral radius values (close to one, considering physically undamped models) in the important low-frequency range. Benchmark analyses are conducted at the end of this study to demonstrate the technique's effectiveness taking into account theoretical problems and complex models that are representative of real-world applications in the OIL & GAS industry.*

1 INTRODUCTION

Wave propagation models are governed by equations that require both spatial and temporal discretization for numerical solutions. Typically, the space and time domains are treated separately, with spatial discretization performed first, generating a semi-discrete time-domain system of equations. This system is then solved using a time-marching procedure [1]. Finite element formulations based on local approximations, for example, have been successfully used in engineering to solve various problems based on partial differential equations. While local approaches are widely explored in spatial discretization, they are less common for time integration, usually relying only on the temporal and/or spatial definition of the time-step value (as in some adaptive time-stepping techniques and multi-time-step/sub-cycling procedures).

To advance on the development of locally defined time-marching formulations, this work studies a truly-explicit time-integration procedure with self-adjustable time integrators, combined with adaptive time-steps/sub-cycling procedures [2]. This approach allows for an effective time-domain solution method where time-steps and time-integration parameters are adaptively and locally computed based on the adopted spatial discretization and model properties. This fully automated formulation requires no user intervention, making it highly suitable for commercial applications.

The discussed approach is second-order accurate, truly explicit, self-starting, and provides extended stability limits and advanced controllable algorithmic dissipation. Over the past decades, various time-integration algorithms have been developed to introduce controllable numerical dissipation to eliminate spurious high-frequency contributions. The intensity of this algorithmic dissipation may be determined by analysing the spectral radius of the time-marching method, which ranges from 0 to 1, with 1 indicating a non-dissipative algorithm. For spectral radii close to zero, spurious frequencies are efficiently eliminated. Many implicit time-marching procedures with dissipative properties have been reported in the literature [1]; however, algorithmic dissipation is also crucial for explicit time-marching algorithms.

The approach that is discussed here introduces time-integration parameters that are locally defined according to the spatially discretized model properties, enhancing the accuracy and stability of the solution. These parameters consider numerical dissipative aspects to quickly dissipate spurious high modes while minimally affecting important low-frequency modes, resulting in a very accurate dissipative time-marching technique. The time-integration parameters are also function of the adopted time-step size and, by considering multiple time-step values (as in this work), these parameters may be better evaluated, improving the solution's effectiveness.

In truly explicit approaches, the method's effective matrices are calculated solely based on the mass matrix, avoiding any solver procedures for algebraic systems of equations if lumped mass matrices are regarded (even if non-diagonal damping matrices are considered). However, the stability limit of truly explicit methods depends on the adopted material damping, often requiring lower time-step values for stability when physical damping is applied. This can lead to inefficient calculations. Nevertheless, the solution methodology described in this work addresses these challenges, allowing for relatively high time-step values even in the presence of conventional material damping.

The present work is structured as follows: first, the governing equation of a generic spatially discretized wave propagation model is presented, followed by the description of the focused

time-integration formulation and subdomain/sub-cycling splitting procedures, detailing the developed automated solution algorithm. Subsequently, numerical applications are provided to showcase the good accuracy and efficacy of the reported procedure. Finally, conclusions are drawn, summarizing the numerous positive attributes of the discussed methodology.

2 GOVERNING EQUATIONS AND TIME INTEGRATION STRATEGY

The set of equations that govern a semi-discrete elastodynamic model can be expressed as:

$$\mathbf{M}\ddot{\mathbf{U}}(t) + \mathbf{C}\dot{\mathbf{U}}(t) + \mathbf{K}\mathbf{U}(t) = \mathbf{F}(t) \tag{1}$$

where $\mathbf{M}$, $\mathbf{C}$, and $\mathbf{K}$ stand for the mass, damping, and stiffness matrix, respectively. The acceleration, velocity, and displacement of the system are represented by vectors $\ddot{\mathbf{U}}(\mathrm{t})$, $\dot{\mathbf{U}}(\mathrm{t})$ and $\mathbf{U}(\mathrm{t})$, respectively, while the applied external force is represented by vector $\mathbf{F}(\mathrm{t})$. The initial conditions are defined as $\mathbf{U}^0 = \mathbf{U}(0)$ and $\dot{\mathbf{U}}^0 = \dot{\mathbf{U}}(0)$, representing the initial displacement and velocity vectors, respectively. In this work, we focus on using lumped mass matrices to define the discretized model, as usual in explicit formulations. This approach avoids solving systems of equations when employing truly explicit time-marching formulations, leading to significantly more efficient analyses. Additionally, we consider classical Rayleigh damping, where the viscous damping matrix $\mathbf{C}$ is assumed to be proportional to the mass and stiffness matrices of the model (i.e., $\mathbf{C} = \alpha_\mathrm{m}\mathbf{M} + \alpha_\mathrm{k}\mathbf{K}$, where α_m and α_k are constants of proportionality).

The time-integration procedure discussed here extends the first methodology presented by Soares [3], who proposed three truly explicit time-marching procedures for the semi-discrete system of equations (1), which use appropriate coefficients and chained compositions of stiffness and damping matrix multiplications to develop efficient second-, third-, and fourth-order accurate time-domain solutions. The present time-integration procedure can be defined by the following recurrence relationships:

$$\mathbf{M}\mathbf{V}_1 = \int_{t^n}^{t^{n+1}} \mathbf{F}(\mathrm{t})\,\mathrm{dt} - \Delta\mathrm{t}[\mathbf{C}\dot{\mathbf{U}}^{\mathrm{n}} + \mathbf{K}(\mathbf{U}^{\mathrm{n}} + \tfrac{1}{2}\Delta\mathrm{t}\dot{\mathbf{U}}^{\mathrm{n}})] \tag{2a}$$

$$\mathbf{M}\mathbf{V}_2 = \Delta\mathrm{t}\mathbf{C}\mathbf{V}_1 \tag{2b}$$

$$\dot{\mathbf{U}}^{\mathrm{n+1}} = \dot{\mathbf{U}}^{\mathrm{n}} + \mathbf{V}_1 - \tfrac{1}{2}\mathbf{V}_2 \tag{2c}$$

$$\mathbf{M}\mathbf{V}_3 = \Delta\mathrm{t}\mathbf{K}(\mu_1\Delta\mathrm{t}\dot{\mathbf{U}}^{\mathrm{n+1}} + \mu_2\Delta\mathrm{t}\dot{\mathbf{U}}^{\mathrm{n}}) \tag{2d}$$

$$\mathbf{U}^{\mathrm{n+1}} = \mathbf{U}^{\mathrm{n}} + \tfrac{1}{2}\Delta\mathrm{t}(\dot{\mathbf{U}}^{\mathrm{n}} + \dot{\mathbf{U}}^{\mathrm{n+1}} - \mathbf{V}_3) \tag{2e}$$

where $\Delta\mathrm{t}$ represents the time-step of the analysis, and the auxiliary vectors $\mathbf{V}_1$, $\mathbf{V}_2$ and $\mathbf{V}_3$ are defined by equations (2a), (2b), and (2d), respectively. The auxiliary vector $\mathbf{V}_3$ is evaluated at the element level, incorporating the local features of the spatially discretized model, which are considered when locally computing the time-integration parameters μ_1 and μ_2. At the element level, a local vector $\mathbf{V}_\mathrm{e}$ is computed as $\mathbf{V}_\mathrm{e} = \mathbf{K}_\mathrm{e}(\bar{\mu}_1^e\dot{\mathbf{U}}_e^{\mathrm{n+1}} + \bar{\mu}_2^e\dot{\mathbf{U}}_e^{\mathrm{n}})$, where the subscripts and superscripts "e" indicate that the variables are defined at an element level (with $\bar{\mu}_i^e = \Delta\mathrm{t}\,\mu_i^e$). The vector $\mathbf{V}$ is assembled by composing $\mathbf{V}_\mathrm{e}$, and $\mathbf{V}_3$ is finally computed as $\mathbf{V}_3 = \Delta\mathrm{t}\mathbf{M}^{-1}\mathbf{V}$, following equation (2d). This locally defined approach allows for the specification of μ_1 and

μ_2 for each element of the discretized model, resulting in a more effective solution procedure.

In this work, the following expressions are used to define μ_1^e and μ_2^e:

$$\mu_1^e = 4(\xi_e\Omega_e^{max} - 1)^{-1}\Omega_e^{max-4} + 4\xi_e\Omega_e^{max-3} + 2\Omega_e^{max-2} \quad (3a)$$

$$\mu_2^e = -2(\xi_e\Omega_e^{max} - 1)^{-1}\Omega_e^{max-4} - 4\xi_e\Omega_e^{max-3} \quad (3b)$$

where $\Omega_e^{max} = \omega_e^{max}\Delta t$ and $\xi_e = \alpha_m(2\omega_e^{max})^{-1} + \frac{1}{2}\alpha_k\omega_e^{max}$ are defined as the maximal sampling frequency and damping ratio of element "e", respectively, with ω_e^{max} representing the highest natural frequency of the element. Expressions (3a-b) are formulated to nullify the spectral radius of the method at Ω_e^{max}, providing maximal numerical damping at the highest sampling frequency of the element. This design optimizes the formulation to reduce the influence of spurious high-frequency modes, enhancing the effectiveness of the analysis. The goal of introducing numerical damping is to eliminate non-physical spurious oscillations caused by unresolved modes. However, designing a dissipative algorithm that introduces high-frequency dissipation without affecting low-frequency modes is challenging. The described methodology adapts by enforcing low and relatively high spectral radius values at the highest and at the important low frequencies of the model, respectively.

When non-zero values of α_k are used, physical damping is already incorporated at the highest frequencies of the model. Therefore, there is no need to introduce additional numerical damping, and $\mu_1^e = \mu_2^e = 0$ can be adopted, which eliminates the need to evaluate equation (2d), enhancing the efficiency of the solution algorithm. In this study, if $\xi_e \geq 0.222$, numerical damping is not applied, and the time integration parameters are set to zero (i.e., $\mu_1^e = \mu_2^e = 0$). In this case, the limiting time-step value for stability, for each element, may be defined as:

$$\text{if } \xi_e \leq 0.222, \qquad \Delta t_e = (2 + 2^{1/2})(\omega_e^{max})^{-1} \quad (4a)$$

$$\text{if } \xi_e > 0.222, \qquad \Delta t_e = (\xi_e\omega_e^{max})^{-1} \quad (4b)$$

As can be seen from equations (4a-b), the discussed technique allows for an easy estimation of the limiting time-step value, which is not common in standard truly explicit approaches. This estimation is important for the automated subdomain divisions and adaptive computations of local time-step values, as it is discussed next. Finally, a minimal value of Ω_e^{max} in equations (3a-b) is suggested to avoid excessive numerical damping when subdomain/sub-cycling splitting procedures are not considered, and a value of $2^{1/2}$ may then be recommended.

2.1 SUB-CYCLING

Sub-cycling is a technique proposed by Belytschko et al. [4] that decomposes a domain into subdomains associated with computations at several "sub-steps." This approach enables an explicit time-marching solution without restricting the entire domain to its shortest critical time-step value, allowing for greater time-step values in different subdomains and reducing computational efforts. The need for sub-cycling arises in problems where meshes include both relatively stiff and soft subdomains, necessitating an overly small time-step value for the entire model. In these cases, to enable efficient computations, it is essential to solve these regions

separately with different time-step values for different subdomains and then integrate the computed responses. However, excessive subdivisions can lead to a decline in both accuracy and efficiency, highlighting the importance of proper sub-cycling considerations.

This study considers an automated algorithm to subdivide the model domain, enhancing efficiency without compromising accuracy. The algorithm performs a controlled subdivision of the domain, computing and assigning a time-step value for each node of the model. The procedure involves grouping elements that can share the same Δt based on their stability limit. By doing so, the model is divided into subdomains, each with different time-step values, allowing for an efficient and accurate solution.

The following sequence of commands is used here to automatically define this subdomain division: (i) calculate the limiting time-steps of all elements (i.e., Δt_e) following equations (4a-b), finding the smallest Δt_e of the model (i.e., Δt_e^{min}, where $\Delta t_e^{min} = \min(\Delta t_e)$), which is the basic time-step for the proposed controlled subdivision of the domain; (ii) with Δt_e^{min} defined, calculate subsequent time-step values as multiple of the power of 2 of this minimal time-step value (i.e., calculate Δt_i, where $\Delta t_i = 2^{(i-1)}\Delta t_e^{min}$); (iii) associate each element to a computed time-step value (i.e., to Δt_i, where $\Delta t_i \leq \Delta t_e \leq \Delta t_{i+1}$ and i indicates the subdomain of that element); (iv) associate a time-step value (i.e., associate a subdomain) to each degree of freedom of the model considering the lowest time-step value of its surrounding elements.

After implementing this subdomain division, it may be necessary to interpolate displacement and velocity values near the boundaries of the time-step subdomains, within the time-marching sub-cycling algorithm. This work employs the following expressions for these interpolations:

$$\mathbf{U}(t) = \frac{1}{2\Delta t}\left(\dot{\mathbf{U}}^{n+1} - \dot{\mathbf{U}}^{n}\right)t^2 + \dot{\mathbf{U}}^{n}t + \mathbf{U}^{n} \tag{5a}$$

$$\dot{\mathbf{U}}(t) = \frac{1}{\Delta t}\left(\dot{\mathbf{U}}^{n+1} - \dot{\mathbf{U}}^{n}\right)t + \dot{\mathbf{U}}^{n} \tag{5b}$$

where t is the current increment of time ($0 \leq t \leq \Delta t$) for the focused subdomain and Δt is the time-step value of the degree of freedom being interpolated, which is related to the neighboring subdomain. A similar expression to equation (5b) is used to interpolate $\mathbf{V}_1$, if required, based on equation (2b).

3 NUMERICAL EXAMPLES

This study evaluates the performance of the reported solution procedure using two elastodynamic applications. In the first application, a homogeneous infinite model is studied, whose analytical solution is known as the Green's function of the elastodynamic problem [5]. The second example is a synthetic model with a complexity level similar to real geological applications, demonstrating the efficacy of the proposed methodology for analyzing large-scale geophysical problems, such as those encountered in the OIL & GAS industry.

The results obtained by the discussed adaptive formulation, both with (referred here as "New/sub") and without (referred here as "New") multi-time-steps/sub-cycling splitting procedures, are compared to those of standard explicit approaches. These standard approaches include the classic Central Difference (CD) method, the explicit generalized α (EG-α) method developed by Hulbert and Chung [6] (where ρb = 0.3665 is adopted, as recommended by the authors to minimize period elongation errors), and the Noh-Bathe (NB) method [7] (where p =

0.54 is adopted, as also recommended by the authors). For each technique, the maximum possible time-step value for stability is applied (considering an element-level evaluation), enabling the most efficient analysis for each approach.

For computing the errors of the calculated responses, when analytical solutions are available, the following expression is adopted:

$$\text{Error} = \left[\sum_{n=1}^{N}\left(u^n - u_A(t^n)\right)^2 \Big/ \sum_{n=1}^{N}\left(u_A(t^n)\right)^2\right] \tag{6}$$

where u stands for the computed field (representing the time history of a degree of freedom), u_A corresponds to its analytical counterpart, and N stands for the total number of time steps in the analysis. In all the analyses that follow, the standard Finite Element Method (FEM) is adopted for the spatial discretization, although the discussed formulation is not restricted to be applied regarding this spatial discretization technique.

3.1 Example 1

In this first example, an infinite homogeneous elastodynamic problem, with three different material damping configurations under an impulsive load in the x direction, is analysed. Initially, we consider (i) null values for α_m and α_k to define a physically undamped configuration. Subsequently, we examine two damped configurations: (ii) $\alpha_m = 1$ and $\alpha_k = 0.000075$ (model 1) and (iii) $\alpha_m = 1$ and $\alpha_k = 0.00045$ (model 2). The model's physical properties are $E = 10\text{KN/m}^2$ (Young's modulus), $\nu = 0$ (Poisson ratio) and $\rho = 10\text{Kg/m}^3$ (mass density). The discretized domain is a circle centered at the load application point, with a higher concentration of elements in the central area. Five FEM meshes, composed of linear triangular elements, are used to discretize the model, each characterized by a specific refinement level: (i) discretization 1: 25,600 elements; (ii) discretization 2: 57,600 elements; (iii) discretization 3: 129,600 elements; (iv) discretization 4: 230,400 elements; (v) discretization 5: 409,600 elements.

Fig. 1 shows the computed adaptive parameters of the proposed methodology for discretization 5. The Δt_e values are indicated in Fig. 1(a), the resulting Δt values per time-marching subdomain are described in Fig. 1(b), and the time-integration parameters μ_1 and μ_2 are depicted in Figs. 1(c-f), with and without time-marching subdomains. As observed in Fig. 1(b), after the automatic subdivision, three time-step subdomains are established for discretization 5, with most of the domain marching with the largest computed Δt value, enabling more efficient analyses using the proposed multi-time-step adaptive formulation.

Time-history results for the computed displacements in the x direction, considering all the above-mentioned time-integration procedures, are depicted in Fig. 2 for discretization 5, at a point located 1.01 m horizontally away from the applied load. In Fig. 3, the computed results along the discretized model for discretization 5, at t=0.45 s, are shown. These figures illustrate that the proposed methodology provides significantly more accurate responses than standard techniques and more effectively dissipates spurious numerical oscillations.

Tab. 1 describes the performance of each adopted solution technique for each spatial discretization. The discussed methodology produces the smallest errors and CPU times, providing the most accurate and efficient time-marching solution procedure. Additionally, as

observed in this table, better results are achieved when multi-time-step/sub-cycling splitting approaches are applied, as these procedures allow more appropriate time-integration parameters to be locally computed for the adaptive methodology. Fig. 4 shows the convergence curves for each selected time-integration procedure, indicating that the discussed technique (with or without sub-cycling calculations) provides lower errors for discretization 1 than the standard techniques do for the much more refined discretization 4, highlighting the considerable superior performance of the novel formulation.

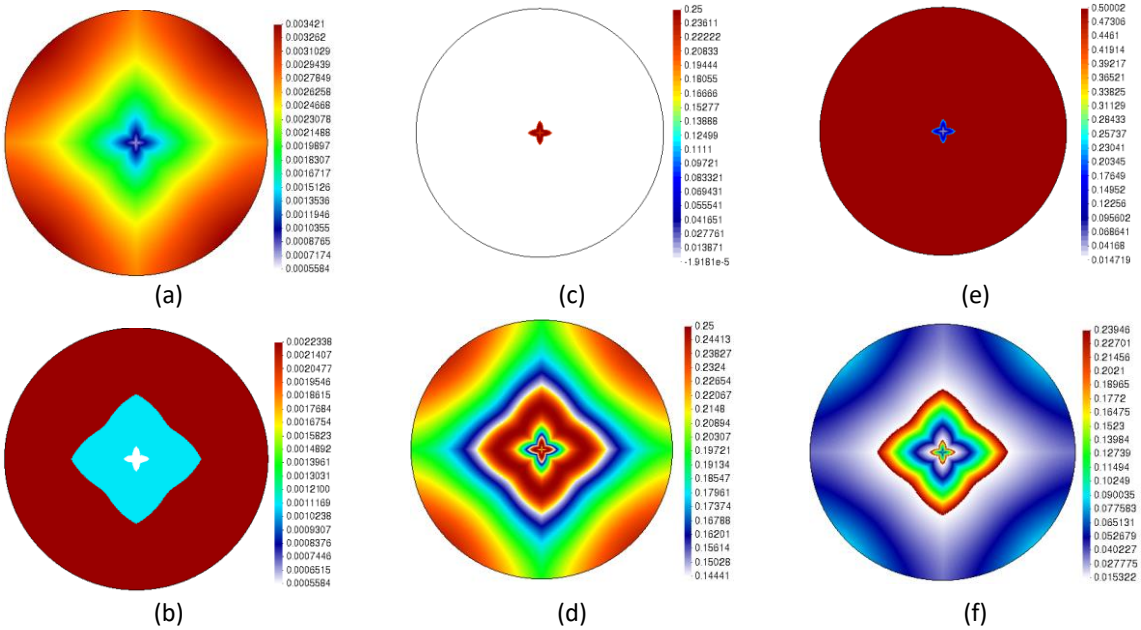

Figure 1: Adaptive parameters along the discretized model, for discretization 5: (a) Δt_e; (b) Δt per time-marching subdomain; (c) μ_1 without considering time-marching subdomains; (d) μ_1 considering time-marching subdomains; (e) μ_2 without considering time-marching subdomains; (f) μ_2 considering time-marching subdomains.

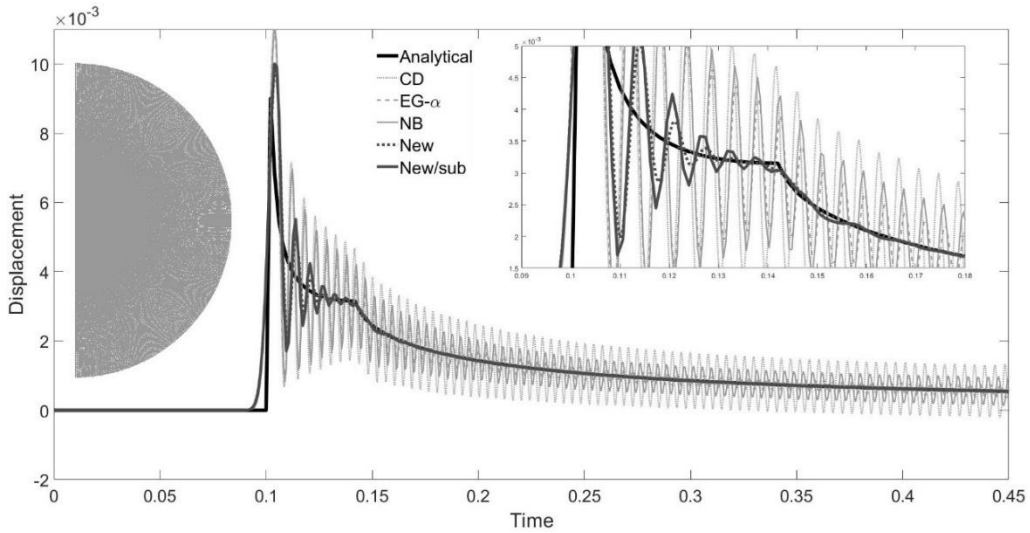

Figure 2: Time history results for discretization 5.

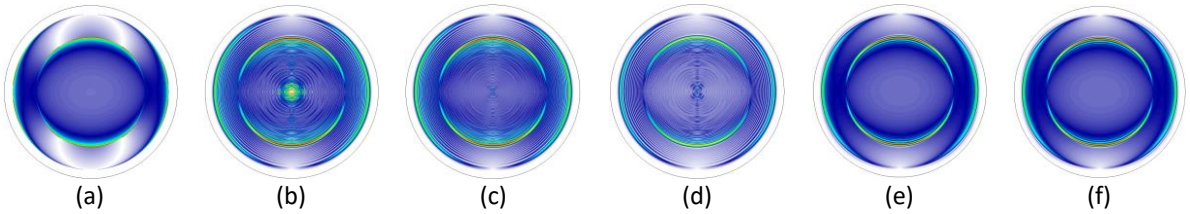

Figure 3: Computed results along the discretized model (discretization 5), at t = 0.45s: (a) analytical; (b) CD; (c) EG-α; (d) NB; (e) new and (f) new/sub.

Table 1: Performance of the methods for the first example (undamped model) [a]

Discretization	Method	Δt (10^{-3}s)	Error (10^{-2})	CPU Time (s)
1	CD	1.278 (1.10)	1.68 (2.55)	23.5 (3.01)
	EG-α	1.152 (1.00)	1.38 (2.10)	26.4 (3.38)
	NB	2.393 (2.07)	1.60 (2.43)	27.3 (3.50)
	New	2.297 (1.99)	0.78 (1.18)	18.4 (2.35)
	New/sub	9.188[b] (7.97)	0.66 (1.00)	7.8 (1.00)
2	CD	0.722 (1.10)	1.59 (2.63)	95.2 (3.13)
	EG-α	0.650 (1.00)	1.29 (2.14)	101.6 (3.34)
	NB	1.352 (2.07)	1.50 (2.49)	103.7 (3.41)
	New	1.297 (1.99)	0.71 (1.18)	74.8 (2.46)
	New/sub	5.191[b] (7.97)	0.60 (1.00)	30.4 (1.00)
3	CD	0.720 (1.10)	1.42 (2.49)	209.3 (3.04)
	EG-α	0.649 (1.00)	1.07 (1.88)	235.7 (3.42)
	NB	1.349 (2.07)	1.32 (2.32)	237.2 (3,44)
	New	1.294 (1.99)	0.63 (1.11)	164.2 (2.38)
	New/sub	5.179[b] (7.97)	0.56 (1.00)	68.8 (1.00)
4	CD	0.563 (1.10)	0.98 (2.35)	261.2 (3.12)
	EG-α	0.508 (1.00)	0.82 (1.96)	290.8 (3.47)
	NB	1.055 (2.07)	0.96 (2.29)	293.1 (3.50)
	New	1.012 (1.99)	0.43 (1.27)	207.3 (2.47)
	New/sub	4.051[b] (7.97)	0.41 (1.00)	83.7 (1.00)
5	CD	0.310 (1.10)	0.46 (2.76)	791.9 (5.08)
	EG-α	0.280 (1.00)	0.30 (1.84)	860.4 (5.52)
	NB	0.581 (2.07)	0.42 (2.54)	890.1 (5.69)
	New	0.558 (1.99)	0.19 (1.16)	536.7 (3.43)
	New/sub	2.233[b] (7.97)	0.17 (1.00)	156.3 (1.00)

[a] Relative values are provided in parenthesis; [b] Maximal Δt in the multiple time-steps analysis.

As previously remarked, two damped configurations for this homogeneous model are also studied in this example to explore other important features of the discussed truly-explicit approach. For these damped configurations, the computed time-step values along the discretized domain are depicted in Fig. 5 for discretization 5. Comparing Figs. 5(a1-b1) and 1(a-b) shows that the proposed technique computes larger time-step values for model 1 (i.e.,

$\alpha_m = 1$ and $\alpha_k = 0.000075$) than for the equivalent undamped model (i.e., $\alpha_m = \alpha_k = 0$), indicating that the novel truly-explicit procedure can enable higher stability limits when physical damping is applied. However, it may also result in reduced time-step values with intense physical damping, as in model 2 (i.e., $\alpha_m = 1$ and $\alpha_k = 0.00045$), which is depicted in Fig. 5(a2-b2). Nevertheless, when a small Δt_e^{min} is evaluated, the discussed multi-time-step/sub-cycling splitting procedure establishes more time-marching subdomains for the model (as illustrated in Fig. 5(b2)), compensating for the increased computational effort associated to a low Δt_e^{min}. Tab. 2 describes the performances of the selected time-integration procedures for these two damped configurations. As indicated, for physically damped models, the novel approach can provide even more efficient analyses than standard truly-explicit techniques, further emphasizing the great effectiveness of the proposed solution procedure.

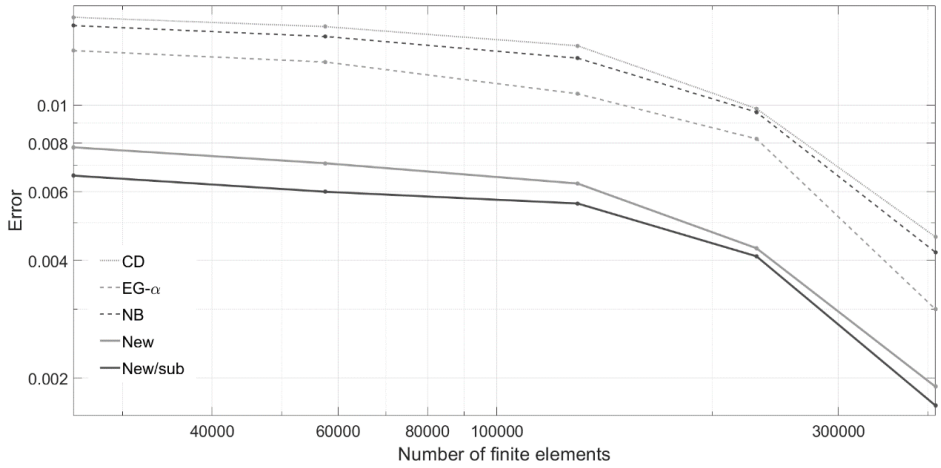

Figure 4: Convergence curves for the selected time-marching procedures and discretizations.

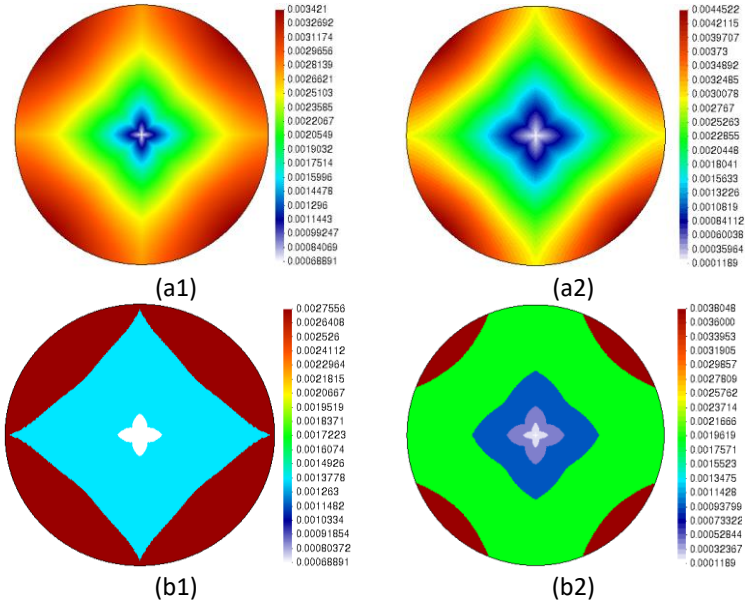

Figure 5: Adaptive time-step values along the discretized model, for discretization 5: (a) Δt_e; (b) Δt per time-marching subdomain; (1) damped model 1; (2) damped model 2.

Table 2: Performance of the methods considering different damped configurations for the first example [a]

Model	Method	Δt (10^{-3}s)	CPU Time (s)
1	EG-α	0.117 (1.00)	1379 (10.52)
	NB	0.428 (3.63)	948 (7.23)
	New	0.688 (5.84)	367 (2.80)
	New/sub	2.755[b] (23.37)	131 (1.00)
2	EG-α	0.029 (1.00)	3593 (13.16)
	NB	0.122 (4.16)	2559 (9.37)
	New	0.118 (4.04)	1225 (4.48)
	New/sub	3.804[b] (129.41)	273 (1.00)

[a] Relative values are provided in parenthesis; [b] Maximal Δt in the multiple time-steps analysis.

3.2 Example 2

The second example considers a geophysical model generated in SEAM, simulating a realistic soil of a salt region in the Gulf of Mexico, complete with stratigraphy that includes oil and gas reservoirs [8]. All model properties are derived from fundamental rock properties, which exhibit subtle contrasts at the macro-layer boundaries, generating realistic synthetic data.

The model, depicted in Fig. 6(a), covers an area of 35 km x 15 km and is discretized using a mesh of 717,139 linear triangular elements. A pulse is applied to its surface at x=17.44 km. The salt regions are described with finer discretizations than the earth layers. Four Δt subdomains were automatically established, as shown in Fig. 6(b). Figures 6(c-d) illustrate the μ_1^e and μ_2^e parameters calculated throughout the model.

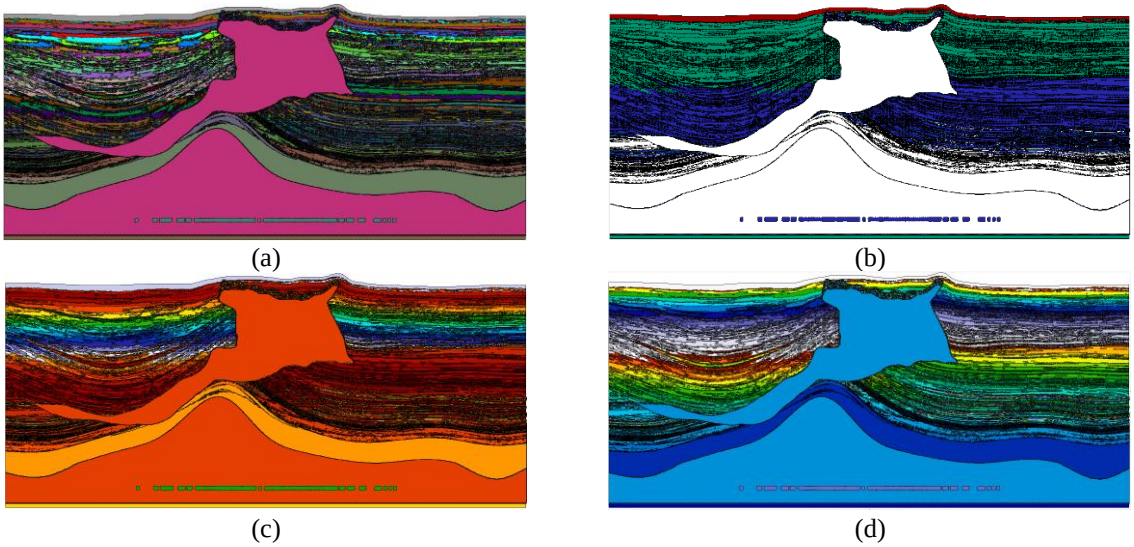

(a) (b) (c) (d)

Figure 6: Geological model: (a) layers illustrating its different physical properties; (b) layers illustrating the computed different time-marching subdomains; and computed time-integration parameters (c) μ_1^e and (d) μ_2^e.

Table 3 presents the performance of the selected time-integration techniques for this model. The discussed adaptive methodology consistently outperforms the selected standard procedures

in terms of CPU time, providing a more efficient approach. Displacement results (in modulus), which are computed using the explicit generalized α method and the adaptive technique with multi-time-steps/sub-cycling splitting procedures, are shown in Fig. 7 considering a logarithmic scale, for better visualization. This figure demonstrates that the reported methodology produces results similar to those of the EG-α method, with the added benefit of fewer spurious oscillations in its computed responses.

Table 3: Performance of the methods for application 2

Method	Δt (10^{-3}s)	CPU Time (s)
CD	2.317(1.10)	831 (3.37)
EG-α	1.983 (1.00)	851 (3.46)
NB	4.338 (2.07)	891 (3.62)
New	4.155 (1.99)	673 (2.73)
New/sub	33.146b (15.96)	246 (1.00)

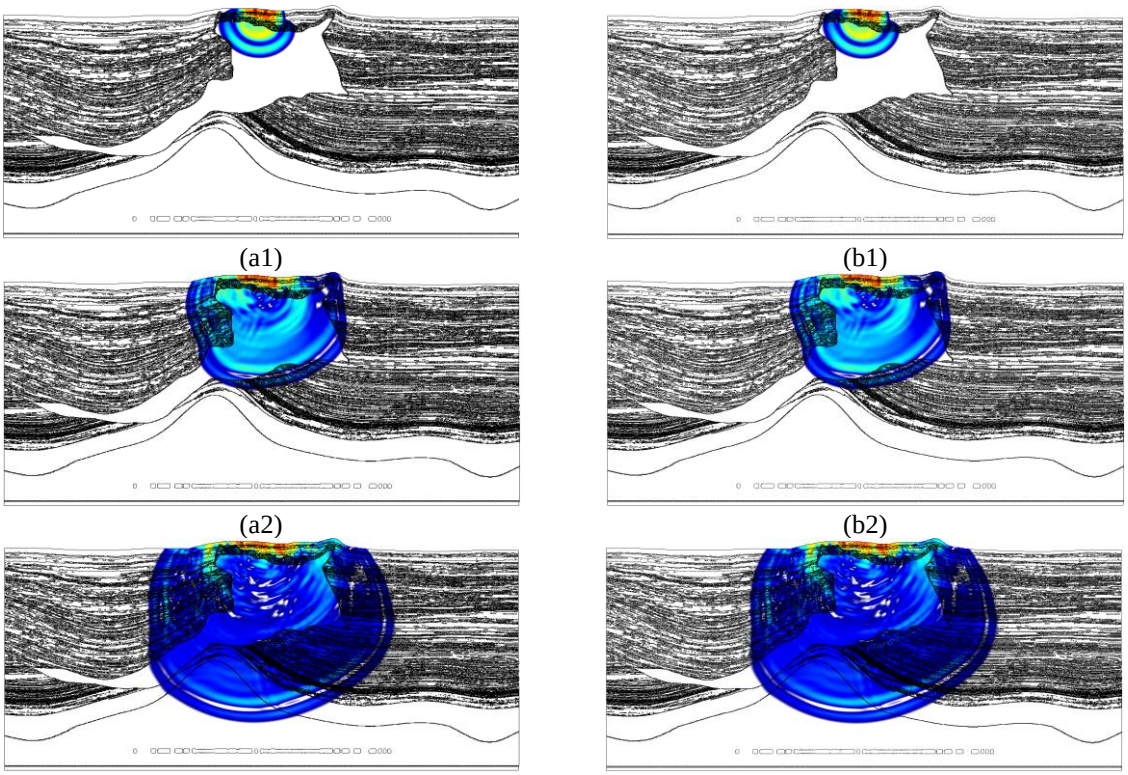

(a1) (b1) (a2) (b2) (a3) (b3)

Figure 7: Computed results for the (a) EG-α and (b) new/sub, at different time instants: (1) 1s; (2) 2s; (3) 3s.

4 CONCLUSIONS

This study discusses an explicit time-marching technique that incorporates subdomain/sub-cycling splitting procedures for solving elastodynamic models. The time-steps and time-integration parameters are automatically and locally determined based on the characteristics of the spatially discretized model. The features of this formulation can be summarized as follows:

(i) it stands as a truly explicit approach that does not require solving a system of equations, as it utilizes lumped mass matrices; (ii) it is based on simple single-step displacement-velocity relations, making it a truly self-starting formulation; (iii) it allows for advanced controllable algorithmic dissipation through optimized, adaptive, locally computed parameters; (iv) it establishes a connection between the adopted temporal and spatial discretization methods, enabling better error balancing; (v) it provides extended stability limits that may not be reduced by the introduction of physical damping (as in usual truly-explicit techniques); (vi) it is entirely automated and simple to apply, requiring no user effort or expertise; (vii) it is highly accurate and efficient, offering more effective analyses when combined with the developed subdomain/sub-cycling splitting procedures.

As illustrated in this paper, the discussed technique is highly versatile and provides effective analyses, consistently outperforming standard time-marching methods. The studied applications demonstrate the robustness of the technique in adapting to the model's properties and its ability to handle complex and highly refined large-scale problems, significantly reducing the related computational burden. In fact, the reported methodology stands as a very effective time-marching technique, making it an attractive option for solving complex wave propagation problems.

Acknowledgements. *The authors acknowledge the support of the Human Resources Program of Agência Nacional do Petróleo, Gás Natural e Biocombustíveis – PRH-9.1/ANP, maintained with resources from the RD&I Clause of Resolution ANP nº 50/2015, CNPq (Conselho Nacional de Desenvolvimento Científico e Tecnológico), and PETROBRAS (CENPES 21066).*

REFERENCES

[1] Tamma, K. K., Zhou, X., & Sha, D. The time dimension: a theory towards the evolution, classification, characterization and design of computational algorithms for transient/dynamic applications. *Archives of Computational Methods in Engineering*, 7, 67-290 (2000).

[2] Soares Jr, D., Pinto, L. R., & Mansur, W. J. A truly-explicit time-marching formulation for elastodynamic analyses considering locally-adaptive time-integration parameters and time-step values. *International Journal of Solids and Structures*,271, (2023) 112260.

[3] Soares Jr, D. Three novel truly-explicit time-marching procedures considering adaptive dissipation control. *Engineering with Computers* 38(4), (2022) 3251-3268.

[4] Belytschko, T., Smolinski, P., & Liu, W. K. Stability of multi-time step partitioned integrators for first-order finite element systems. *Computer Methods in Applied Mechanics and Engineering*, 49(3), (1985) 281-297.

[5] Mansur, W. J. *A time-stepping technique to solve wave propagation problems using the boundary element method* (Doctoral dissertation, University of Southampton) (1983).

[6] Hulbert, G. M., & Chung, J. Explicit time integration algorithms for structural dynamics with optimal numerical dissipation. *Computer Methods in Applied Mechanics and Engineering*, 137(2), (1996) 175-188.

[7] Noh, G., & Bathe, K. J. An explicit time integration scheme for the analysis of wave propagations. *Computers & structures*, 129, (2013) 178-193.

[8] Fehler, M. (2012). SEAM update: SEAM phase I-RPSEA update: Status of simulations. *The Leading Edge*, 31(12), 1424-1426.